J|A|C|S COMMUNICATIONS

Published on Web 07/15/2009

# Transverse-Dephasing Optimized Homonuclear *J*-Decoupling in Solid-State NMR Spectroscopy of Uniformly $^{13}$C-Labeled Proteins

Ségolène Laage,[†] Anne Lesage,[†] Lyndon Emsley,[†] Ivano Bertini,[‡] Isabella C. Felli,[‡] Roberta Pierattelli,[‡] and Guido Pintacuda*[,†]

*Université de Lyon, CNRS/ ENS Lyon/ UCB-Lyon 1, Centre RMN à Très Hauts Champs, 5 rue de la Doua, 69100 Villeurbanne, France, and Department of Chemistry and Magnetic Resonance Center (CERM), University of Florence, Via Luigi Sacconi 6, 50019 Sesto Fiorentino, Florence, Italy*

Received May 1, 2009; E-mail: guido.pintacuda@ens-lyon.fr; ivanobertini@cerm.unifi.it

Resolution in magic angle spinning (MAS) NMR spectra of solid macromolecules has recently greatly improved due to progress in sample preparation, probe and magnet technology, and heteronuclear decoupling performance, thus opening the field to the structural characterization of systems highly pertinent in many areas of modern biology.[1,2] One of the main barriers to reach higher resolution in fully isotopically enriched systems, and even more complex molecules, is the broadening of the $^{13}$C line widths due to homonuclear $^{13}$C−$^{13}$C scalar *J*-couplings.

While *J*-decoupling in the indirect dimension of $^{13}$C MAS spectra can be achieved by constant-time acquisition[3] or by application of semiselective pulses,[4] homonuclear *J*-decoupling in the direct dimension is more problematic. Approaches have been proposed which either rely on the selective irradiation of one spectral region during acquisition[5] or make use of deconvolution and spectral reconstruction.[6] Both solutions can work but have practical disadvantages. For example, the latter scheme relies on postacquisition data processing, while the former imposes stroboscopic detection, which affects the signal-to-noise ratio.

An alternative for homonuclear *J*-decoupling, introduced in MAS NMR[7] and now widely employed in solution NMR,[8,9] makes use of semiselective pulses to detect a single component of the $^{13}$C doublet.[10] This spin-state selection is based on the combination of pure in-phase and pure antiphase coherences, separately recorded in two experiments (IPAP). The scheme relies on a total evolution period of the *J* interaction of 1/2*J* (9.1 ms for, e.g., $J_{COCA} = 55$ Hz). It is therefore only currently practical for the analysis of long-lived carbonyl resonances. Notably, because of long transverse dephasing periods, homonuclear IPAP usually does not achieve the expected gain in sensitivity.

To address this problem, an alternative scheme, dubbed S$^3$E (Spin State Selective Excitation),[11] relies on partial interconversion between in-phase and antiphase components and requires half of the time (1/4*J*, i.e. 4.5 ms for $J_{COCA} = 55$ Hz). This was implemented in solution $^{13}$C NMR[8] and recently improved.[10,12] Here we show how this method can be adapted to NMR of biosolids and illustrate it on a microcrystalline sample of the oxidized superoxide dismutase (SOD),[13] a dimeric paramagnetic enzyme of 32 kDa for which it leads to spectra with significantly improved resolution *and* sensitivity.

Figure 1 (a and b) shows the pulse-sequences for the new spin-state selection filter. The A and B blocks of the experiment differ in the position of the $\pi$ pulses on the I spin, applied either just after creation of I transverse magnetization (A) or after evolution of the scalar coupling at the end of the block (B), when the in-phase and antiphase operators are both present (see Supporting Information (SI)). Therefore the change in position of these $\pi$ pulses, combined with a suitable cycle of the receiver phase, allows the recording of two distinct signals, which are both linear combinations of in-phase and antiphase components. The two doublet components can then be separated by adding and subtracting the acquired signals and subsequent first-order phase correction of 90° of one of the two combinations. These can be combined (after shifting the spectra to the center of the original multiplet by $\pm J/2$ Hz) to remove the splitting and increase the overall signal-to-noise ratio. It is worth noting that, due to its design, the pulse sequence that decouples I from S will at the same time decouple S from I.

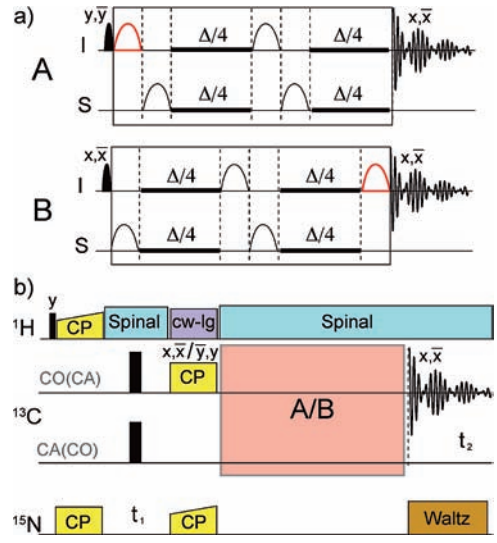


***Figure 1.*** (a) Pulse sequence elements for the S$^3$E filter. The bell shapes represent band selective $\pi$-pulses, and the delay $\Delta/4$ is set to 1/8*J*. $\pi$ pulses are applied either right before or right after the *J* evolution period (in red), and an extra $\pi$-pulse is added at the beginning of the evolution period on the S channel to compensate for transient Bloch−Siegert effects[14] due to the low rf-fields of selective pulses. (b) Pulse sequence for NCO and NCA correlation experiments. Experimental parameters and the extended phase cycles are reported in the SI.

Figure 1b shows how this S$^3$E block can be adapted into conventional solid-state NMR sequences under MAS. In particular, panel 1b illustrates its incorporation into triple-resonance NCO or NCA schemes, which constitute the basis of any biomolecular investigation in MAS NMR.[1] Here homonuclear *J*-decoupling is performed in the direct dimension, while a double $^1$H−$^{15}$N and $^{15}$N−$^{13}$C SPECIFIC CP step[15] is used to selectively drive magnetization onto the $^{13}$C I spin (either CO or CA), and the observed spectrum is labeled in $t_1$ with the $^{15}$N chemical shift.

[†] Université de Lyon.
[‡] University of Florence.



10.1021/ja903542h CCC: $40.75 

Figure 2 shows the resulting 2D spectra, with some extracted rows, compared to the same experiments performed without $S^3E$. In the NCO case (Figure 2a−b; I = CO, S = CA), $S^3E$ efficiency is demonstrated through a gain in resolution (up to a factor of 2.2) and sensitivity (up to a factor of 1.4). Notably, a sensitivity gain is also observed for $^{13}C$ spins sitting closer to the paramagnetic Cu(II) (e.g., Val 81; see SI), while these signals are barely observable with the IPAP scheme. It is worth noting that the resolution provided by this experiment, shown in Figure 2a, enables identification of 145 $^{13}CO$ signals, a result up to now inconceivable for a microcrystalline protein of such large size.

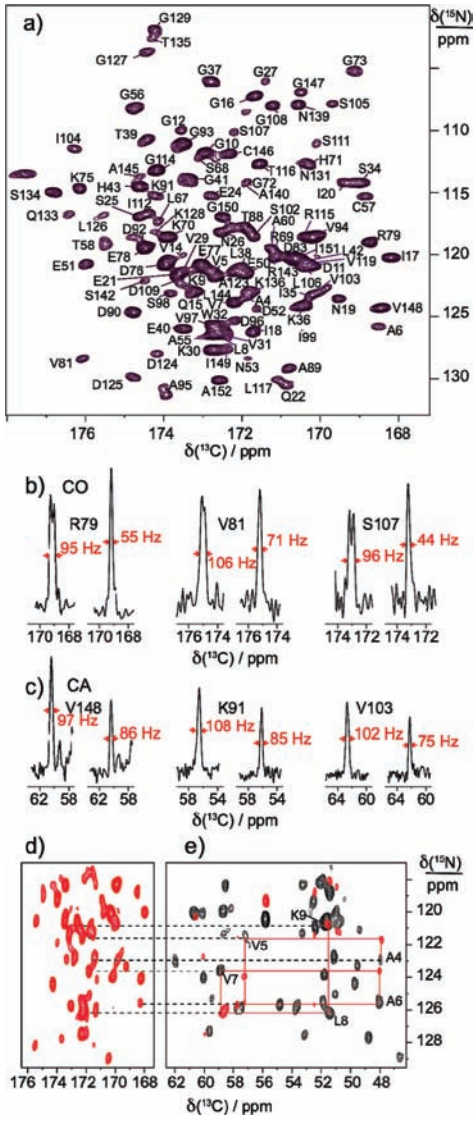


***Figure 2.*** (a) NCO *J*-decoupled spectrum of dimeric, oxidized SOD at 20 kHz MAS (see SI for details). (b−c) Rows extracted from 2D NCO (b) and NCA (c) spectra recorded without (left) or with (right) the $S^3E$ filter. (d−e) NCOCA (in red) and NCA (in black). Red lines indicate sequential walks. Black dotted lines correlate intraresidue CO−CA resonances.

The NCA correlation constitutes a more challenging target, due to the shorter refocused transverse dephasing times, $T_2'$, of CA signals and the additional $^1J$ coupling to CB. However, the $S^3E$ filter still provides a resolution gain with little or no compromise in terms of sensitivity (Figure 2c). Further improvement can be obtained by implementing a double $S^3E$ scheme (two intertwined $S^3E$ blocks)[12] that separates all four spin states of the CA resonance, while the evolution time is set to only 1/4 of the smaller *J* value (not shown). As CA and CB chemical shifts may overlap (Ser, Thr), it is difficult to decouple all residues, but for many signals the gain in resolution is significant.

The property of simultaneous decoupling is particularly attractive when the signals of both coupled nuclei are detected at the same time, which often happens in biomolecular solid-state applications, in contrast to solution ones. For example, $S^3E$ can efficiently be used to obtain a *J*-decoupled NCOCA spectrum (Figure 2d, e), which provides two resolved regions, one for reading the carbonyl resonance, and one for sequentially assigning the backbone (in a sequential walk between NCA and NCOCA as seen in panel (e)).

In conclusion, we have introduced a new experimental approach to *J*-decoupling under MAS, which provides both resolution and sensitivity enhancement for solid-state NMR correlation experiments. The obtained resolution is good enough here to allow unprecedented insight into the NCO and NCA cross peak regions of a large paramagnetic protein. This technique may advantageously be combined with other multidimensional $^{13}C$ detected experiments (see SI for the pulse sequences of $S^3E$-PDSD and 3D $S^3E$-NCOCA as examples) and is expected to be of major interest for solid-state NMR of proteins, as improving spectral resolution is of great practical importance for the site-specific characterization of large biomolecular systems.

**Supporting Information Available:** Experimental details, pulse sequences for $S^3E$-PDSD and 3D $S^3E$-NCOCA, $S^3E$ theory, and comparison with IPAP decoupling. This material is available free of charge via the Internet at http://pubs.acs.org.

**Acknowledgment.** We acknowledge support from the Agence Nationale de la Recherche (ANR 08-BLAN-0035-01), from Ente Cassa di Risparmio di Firenze, and from Joint Research Activity and Access to Research Infrastructures activity in the sixth Framework Program of the EC (RII3-026145, EU-NMR).

## References

(1) McDermott, A. E. *Curr. Opin. Struct. Biol.* **2004**, *14*, 554–561.
(2) (a) Wasmer, C.; Lange, A.; Van Melckebeke, H.; Siemer, A. B.; Riek, R.; Meier, B. H. *Science* **2008**, *319*, 1523–1526. (b) Lange, A.; Giller, K.; Hornig, S.; Martin-Eauclaire, M. F.; Pongs, O.; Becker, S.; Baldus, M. *Nature* **2006**, *440*, 959–962. (c) Böckmann, A. *Angew. Chem.* **2008**, *47*, 6110–6113.
(3) Chen, L. L.; Olsen, R. A.; Elliott, D. W.; Boettcher, J. M.; Zhou, D. H. H.; Rienstra, C. M.; Mueller, L. J. *J. Am. Chem. Soc.* **2006**, *128*, 9992–9993.
(4) Straus, S. K.; Bremi, T.; Ernst, R. R. *Chem. Phys. Lett.* **1996**, *262*, 709–715.
(5) Chevelkov, V.; Chen, Z.; Bermel, W.; Reif, B. *J. Magn. Reson.* **2005**, *172*, 56–62.
(6) Scholz, I.; Jehle, S.; Schmieder, P.; Hiller, M.; Eisenmenger, F.; Oschkinat, H.; van Rossum, B. J. *J. Am. Chem. Soc.* **2007**, *129*, 6682–6683.
(7) (a) Duma, L.; Hediger, S.; Lesage, A.; Emsley, L. *J. Magn. Reson.* **2003**, *164*, 187–195. (b) Duma, L.; Hediger, S.; Brutscher, B.; Böckmann, A.; Emsley, L. *J. Am. Chem. Soc.* **2003**, *125*, 11816–11817. (c) Verel, R.; Manolikas, T.; Siemer, A. B.; Meier, B. H. *J. Magn. Reson.* **2007**, *184*, 322–329.
(8) (a) Bermel, W.; Bertini, I.; Duma, L.; Felli, I. C.; Emsley, L.; Pierattelli, R.; Vasos, P. R. *Angew. Chem.* **2005**, *44*, 3089–3092. (b) Bertini, I.; Felli, I. C.; Kümmerle, R.; Luchinat, C.; Pierattelli, R. *J. Biomol. NMR* **2004**, *30*, 245–251.
(9) Bermel, W.; Bertini, I.; Felli, I. C.; Piccioli, M.; Pierattelli, R. *Prog. Nucl. Magn. Reson. Spectrosc.* **2006**, *48*, 25–45.
(10) Bermel, W.; Felli, I. C.; Kümmerle, R.; Pierattelli, R. *Concepts Magn. Reson. Part A* **2008**, *32A*, 183–200.
(11) (a) Sørensen, M. D.; Meissner, A.; Sørensen, O. W. *J. Biomol. NMR* **1997**, *10*, 181–186. (b) Sørensen, M. D.; Meissner, A.; Sørensen, O. W. *J. Magn. Reson.* **1999**, *137*, 237–242.
(12) Bermel, W.; Bertini, I.; Felli, I. C.; Matzapetakis, M.; Pierattelli, R.; Theil, E. C.; Turano, P. *J. Magn. Reson.* **2007**, *188*, 301–310.
(13) Pintacuda, G.; Giraud, N.; Pierattelli, R.; Böckmann, A.; Bertini, I.; Emsley, L. *Angew. Chem.* **2007**, *46*, 1079–1082.
(14) Emsley, L.; Bodenhausen, G. *Chem. Phys. Lett.* **1990**, *168*, 297–303.
(15) Baldus, M.; Petkova, A. T.; Herzfeld, J.; Griffin, R. G. *Mol. Phys.* **1998**, *95*, 1197–1207.

JA903542H